ACADEMIC PRESS

Available online at www.sciencedirect.com
SCIENCE DIRECT®

Journal of Catalysis 216 (2003) 236–245

JOURNAL OF CATALYSIS

www.elsevier.com/locate/jcat

Surface chemistry and catalysis on well-defined oxide surfaces: nanoscale design bases for single-site heterogeneous catalysts

Mark A. Barteau,[a,*] James E. Lyons,[b] and In K. Song [c]

[a] *237A Colburn Lab., Department of Chemical Engineering, Center for Catalytic Science and Technology, University of Delaware, Newark, DE 19716, USA*
[b] *The Catalyst Group, PO Box 637, Spring House, PA 19477, USA*
[c] *Department of Environmental and Applied Chemical Engineering, Kangnung National University, Kangnung 210-702, South Korea*

Received 17 July 2002; revised 17 September 2002; accepted 22 October 2002

Abstract

As the surface science of metal oxides has developed over the past two decades, it has made increasing contributions to the understanding of the site requirements for catalysis by oxides. Metal oxide single crystals and thin films represent the systems most often studied by surface science techniques as models of oxide catalysts. We explore an alternative approach—molecular functionalization of surfaces with ordered arrays of discrete, reactive oxide molecules. Heteropolyanions (polyoxometalates) can be deposited to form ordered monolayers that permit site-by-site mapping of chemical functions on the surface, as well as characterization of redox properties of individual molecules by tunneling spectroscopy with the scanning tunneling microscope. These nanoscale oxide clusters exhibit negative differential resistance in their tunneling spectra at potentials that track their reduction potentials. Thus tunneling spectroscopy measurements may provide correlation and prediction tools for catalyst performance in selective oxidation processes. Because polyoxometalate monolayers present uniform catalytic sites whose redox properties can be defined by single molecule spectroscopy, they may serve as a prototype of single site heterogeneous catalysts designed and fabricated on the nanoscale.

Keywords: Metal oxides; Heteropolyacids; Polyoxometalates; Scanning tunneling microscopy; Negative differential resistance; Selective oxidation

1. Introduction

1.1. Directions for model oxide catalysts

When assessing directions in catalysis one often focuses on specific chemistries, e.g., alkane activation, olefin polymerization, and alkylation processes. However, it is also worthwhile to consider crosscutting themes, both those behind these that could produce broad advances in catalytic science and technology, and those with the potential to enable new catalytic processes for which the needs and opportunities have not yet been envisioned. Among the latter, the following appear to be of growing importance in this first decade of the 21st century: improvement of atom economy via catalysis, development of catalysts approaching 100% selectivity, and catalysts as devices or integral components of devices.

Advances in catalysis by metal oxides have provided a number of improvements in atom economy. Historical examples include processes such as butane oxidation to maleic anhydride with vanadyl pyrophosphate catalysts, which completely replaced the older benzene oxidation process. Emerging examples include catalysts for applications ranging from water–gas shift [1,2], to methanol oxidation [3–6], to ketene synthesis [7–10]. One of the striking aspects about these emerging applications is their genesis from surface science studies of metal oxides. They provide clear demonstrations that advances in the fundamental understanding of oxide surface chemistry can lead to new catalysis.

If one considers the potential for heterogeneous catalysts to produce selectivities approaching 100%, it is clear that nonmetals, and metal oxides in particular, will be central to such developments. The reason is that, to achieve such selectivities, heterogeneous catalysts will need to share a key characteristic with the homogeneous and biological catalysts that generally offer selectivity advantages—they must present uniform sites (and uniform contact patterns—an additional catalyst engineering constraint). In effect, what will

* Corresponding author.
E-mail address: barteau@che.udel.edu (M.A. Barteau).

0021-9517/03/$ – see front matter
doi:10.1016/S0021-9517(02)00114-8

be required are "single site" heterogeneous catalysts. At metal oxide surfaces, metal cations separated by oxygen anions are intrinsically analogous to mononuclear metal complexes in solution. They offer possibilities of uniformity and site isolation that supported metal catalysts prepared by conventional means cannot. However, to make use of such intrinsic characteristics of oxides, it is essential to define the structure-reactivity relationships for these materials, i.e., to understand the nature of the uniform sites that one wishes to create.

Surface science approaches have provided the tools to expand our knowledge base in just this fashion. They can define surface site requirements, elucidate surface reaction mechanisms, and help to establish analogies to coordination chemistry in solution. Over the past two decades, the field of oxide surface science has come into its own, and the full arsenal of UHV techniques has been applied to a variety of oxide single crystals and thin films. One of us has contributed several reviews examining the progress of metal oxide surface science over this period, and its impact on catalysis [11–14]. Studies of small organic molecules on model oxide surfaces have served to define the requirements for surface chemical reactions, including various acid–base, oxidation, reduction, and coupling processes, in terms of key characteristics of surface sites. These characteristics are cation coordination environment, oxidation state, and redox properties. Still, the studies completed to date provide a rather sparse database for catalyst design. It is difficult, for example, to find results comparing more than a handful of ordered oxide surfaces for even simple C_1 probe molecules. There is still much to be learned in this regard from "traditional" surface science studies of well-defined oxide surfaces.

A critical challenge in utilizing well-ordered single crystals or thin films of metal oxides as models of oxide catalysts is the need to address the chemistry of surface defects. A significant fraction of the catalytic chemistry of oxides may be associated with defect sites. There is a need to characterize these for working catalysts, to synthesize model catalysts with controlled numbers and types of defects, and to characterize the nature and the reactivity of the sites on model surfaces.

Scanning probe microscopies (SPM) represent perhaps the most important family of techniques for advancing our understanding of oxide surface reactivity by addressing these needs. Although atomic resolution SPM studies of oxide surfaces are still not routine, work reported from a number of laboratories to date has shown the ability of these techniques to define surface structures, to highlight surface defects, and to probe the arrangement of adsorbates on oxide surfaces [15–21]. In combination with reaction experiments, vibrational spectroscopies, and other electron spectroscopies, this approach can produce structure-reactivity relations for oxide surfaces, including those for defects and other minority structures deliberately introduced. SPM techniques are not limited to the UHV environment and can provide important insights into the surface structures of both model materials and catalysts under realistic reaction conditions. However, the number of studies connecting atomic resolution SPM with reaction studies on oxides is still quite limited.

It is worthwhile to consider alternatives to single crystals and thin films as planar models of oxide catalysts amenable to scanning probe techniques and surface spectroscopies. Of the three key characteristics of surface sites noted above, cation coordination environment, oxidation state, and redox properties, the tendency is to focus on the first two. Is the structure of the model surface representative of that of a portion of the surface of a high surface area, bulk material? Are representative cation oxidation states present in the model? If so, what chemistry can be connected with these? If one addresses these questions in this order, one is led to focus on atom connectivity (structure), and metal:oxygen ratio as the principal characteristics of the model. An alternative is to consider the use of *molecularly functionalized* (or *molecularly tailored*) surfaces as models of oxide catalysts. In effect one can create ordered structures of uniform, discrete chemical functions as model catalysts. This may permit the characterization of reactive inorganic surfaces at the molecular level; indeed one can hope to connect spectroscopy of surface sites from single molecule measurements directly to catalytic performance. Such systems also promise simple scale up; both low surface area models and high surface area catalysts may in principle take advantage of the same synthetic strategies to create molecularly functionalized surfaces.

Self-assembled organic monolayers have attracted considerable attention over the past decade. In contrast, self-assembled inorganic monolayers, which may provide an entrée into quite different materials properties and applications, have been much less studied. We have utilized discrete metal oxide clusters (heteropolyanions, HPAs, also known as polyoxometalates, POMs) to construct self-assembled monolayers with novel chemical and electronic properties. These HPA monolayers have a host of potential applications, including sensors and other electronic devices, but they may have particularly important applications in catalysis as predictive and practical tools for selective oxidation.

Polyoxometalates are early transition metal oxygen-anion heteropolyanion clusters that exhibit a wide range of molecular architectures, surface charge densities, and chemical and electronic properties. Varying in sizes from about one to a few nanometers, these molecular clusters have found applications as acid and oxidation catalysts [21,22], electrode functionalization agents [23], and antiretroviral agents [24], among others. From a materials perspective, HPA monolayers represent a rich field of opportunity: they are highly ordered, planar materials with complex but highly variable chemical and electronic functions built into each lattice point in the monolayer. One of the great advantages of HPA monolayer assemblies as compared with the more widely studied organic monolayers is the greater thermal stability of HPAs.

This stability makes monolayers of these nanoscale clusters good candidates for applications that may involve severe environments, such as heterogeneous catalysis.

The redox properties of HPAs can be varied dramatically by virtually the entire range of conceivable substitutions. Taking the acid forms of HPAs having the Keggin structure (e.g., $H_3PMo_{12}O_{40}$) as an example, one can exchange other cations for the protons which serve as countercations, one can substitute other metals such as W, V, and Cu into the framework of the heteropolyanion, and one can use heteroatoms such as Si in place of phosphorous. Thus both the acidity of these materials and the redox properties of the heteropolyanion framework can be varied; redox-active transition metals can be introduced as both countercations and as heteropolyanion framework constituents. This considerable versatility within a well-defined structure has led to the application of these materials as homogeneous and/or heterogeneous catalysts for several acid-catalyzed and oxidative conversions of organic molecules [25]. Of particular current interest is their potential for application in the catalysis of alkane conversions [26].

Two experimental discoveries are behind the opportunities for self-assembled monolayers of these nanoscale oxide molecules as model oxide catalysts. First, they form well-ordered monolayers on surfaces such as graphite [27] and silver [28]. Second, they exhibit novel electronic signatures that can be used to identify individual molecules in these monolayers and to predict their redox properties.

We were one of the first two groups to demonstrate that ordered HPA monolayers could be formed on graphite surfaces by deposition from solution and imaged in air with molecular resolution by scanning tunneling microscopy (STM) [29,30]. Tunneling spectroscopy measurements on individual HPA molecules revealed current peaks, referred to as negative differential resistance (NDR), in their current-voltage (I–V) spectra [29,31] as shown in Fig. 1. We have published extensively on our observation of NDR in tunneling spectra of HPA monolayers [29,31–44]. Although quantitative models remain to be developed, NDR is best explained as a consequence of a double-barrier resonant tunneling structure or quantum well in which the electron transmission probability increases at an applied potential corresponding to a resonance (or defect or trap state) energy. In the case of HPAs, it is plausible that the state through which resonant tunneling occurs is the lowest unoccupied molecular orbital of the HPA, since the NDR peaks are observed at negative sample biases whether the HPAs are located on the sample or on the tip [44]. NDR peak voltages can be correlated to the reduction potentials of the HPAs [31–44] and thus can be used to fingerprint different HPAs. The redox properties, and therefore the NDR peak potentials can be varied by changing the central heteroatoms, framework metal atoms, or countercations (which are located at bridging positions between anions in the HPA monolayers [31,37,39,41]). In each of these cases, the trends in NDR voltages correlate well with the electronegativities of the changed constituents [32–42]. Experiments with mixed arrays of polyanions have shown that chemical identity can be distinguished on an individual basis using tunneling spectroscopy, in effect demonstrating one can probe a reactive surface on a *site-by-site* basis [35]. We have also shown for the first time that ordered monolayers can be formed of transition metal salts of HPAs [36]. By coupling redox-active metal centers with redox-active HPAs, one may improve both activity and selectivity for various metal-catalyzed oxidation processes. Previous studies provide precedents for this strategy in terms of catalyst performance [45], but it remains to connect this with molecular level control of surface redox properties that these ordered HPA monolayers suggest is feasible.

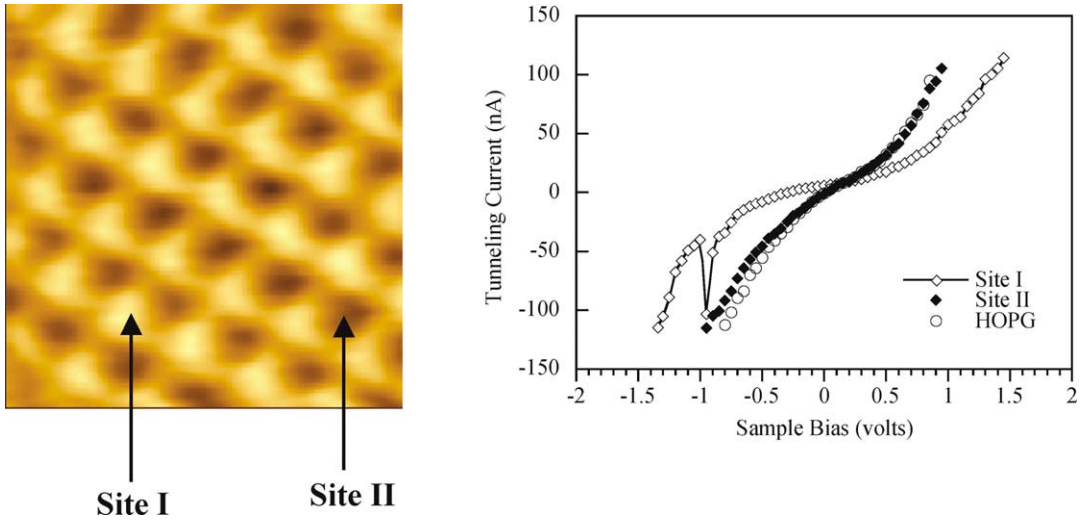

Fig. 1. STM image of $H_3PMo_{12}O_{40}$ array on graphite (image area 5.07 × 5.07 nm), and current-voltage (I–V) spectra taken at two different sites in the STM image, indicating that the array is monolayer. The I–V spectrum at Site I (atop a POM molecule) exhibits NDR at −0.95 V.

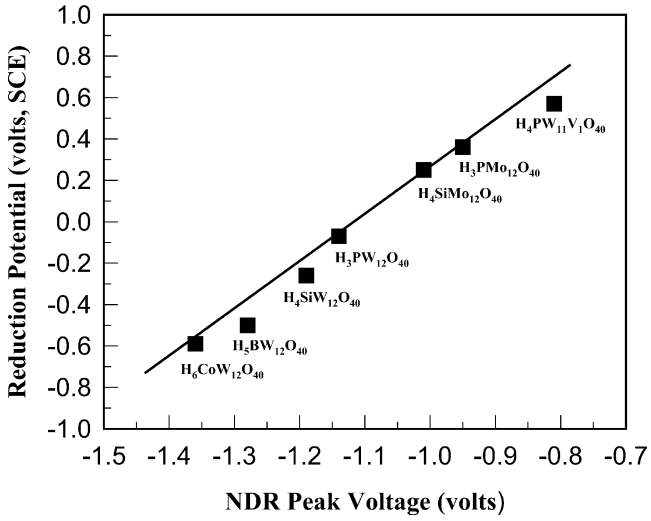

Fig. 2. Correlation between reduction potentials and NDR peak voltages for Keggin ions with different heteroatoms and framework compositions.

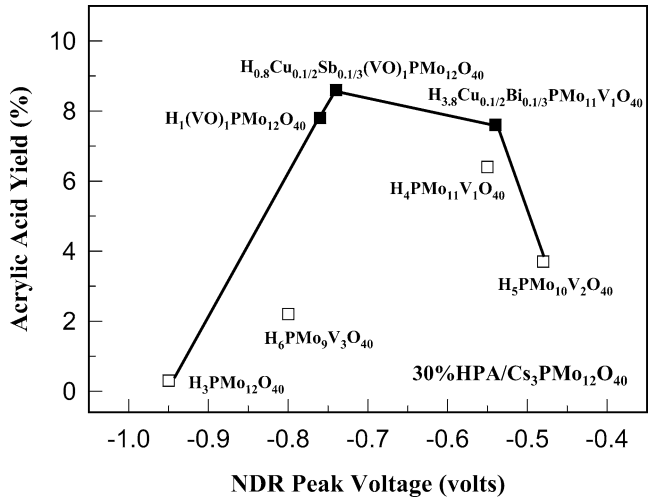

Fig. 3. Acrylic acid yields over supported HPA catalysts, plotted as a function of NDR peak voltage of the HPAs. Oxidations were carried out by first activating the catalyst by flowing 1 atm of a propane/air mixture (52.5/38 ml/min) at 350 °C, then carrying out the oxidation by continuously passing a mixture of propane, air, and nitrogen (3.2/15/16 ml/min) over 4 ml of the catalyst (30% HPA/$Cs_3PMo_{12}O_{40}$ having a medium pore radius of ∼ 120 Å) at 375–380 °C [56]. Open squares denote heteropolyacids; filled squares are HPA catalysts for which some protons have been exchanged.

What we find particularly exciting are the strong correlations that we have been able to develop between the redox properties of HPAs, including reduction potentials from electrochemical measurements, and NDR peak voltages. Fig. 2 illustrates the excellent correlation between reduction potentials and NDR peak voltages for Keggin ions with different heteroatoms and framework transition metal constituents. Reduction potential measurements shown in Fig. 2 were obtained under consistent conditions [46–48]. As we have noted previously, the variation of conditions and of reference electrodes in electrochemical experiments makes it quite difficult to construct a comprehensive scale of HPA reduction potentials from these reports. As we have shown [34], the use of NDR peak potentials circumvents this problem. NDR peak voltages can be measured in air for individual molecules, either in the surface monolayers or deposited on the STM tip [44]. Such a level of surface chemical characterization in principle permits one to map redox active centers site-by-site on model catalyst surfaces in order to develop structure-function relationships for these materials. It also offers the prospect of using single molecule spectra of HPAs in air as predictive tools in oxidation catalysis. For example, Fig. 3 illustrates a comparison of results from the patent literature for selective oxidation of propane to acrylic acid, vs NDR peak voltages measured in our laboratory for the relevant HPA monolayers [34]. These suggest that there is an optimum reduction potential/NDR peak voltage for HPA catalysts for this process—in effect that one might use NDR peak voltages measured with the STM to construct "volcano" plots to correlate and to predict desired oxidation activities.

1.2. Reaction networks in oxidation catalysis

Before one examines correlations of single molecule tunneling spectra with catalytic performance, it is necessary to consider the patterns that one might expect to encounter, and the origins and consequences of each. For example, one most often encounters volcano plots as means to correlate the *activity* of different catalysts for *single* reactions involving two or more elementary steps, with the heat of formation (or its surrogate) of the most abundant reaction intermediate. The "textbook" example is the catalytic decomposition of formic acid on metals: activity initially increases with increasing heat of formation of the metal formate (or the metal oxide as a generic surrogate), passes through a maximum for platinum, and then decreases for metals with progressively higher heats of formation of their formates [49]. The usual explanation is that for metals with heats of formation of the intermediate less than that of the optimum catalyst, formation of the intermediate is rate determining; for metals on the opposite slope of the volcano, reaction of the surface intermediate is rate determining.

The simplest reaction scheme in oxidation catalysis is a two-step redox cycle in which a reactant consumes oxygen of the catalyst, and oxygen is replenished by catalyst reoxidation. One might expect that catalytic activity would increase monotonically with increasing ability of the catalyst to give up oxygen, i.e., with increasing reduction potential. This corresponds to the leg of a volcano plot for which reaction of the catalytic intermediate is rate determining. If there is a shift in the rate determining step on catalysts that bind oxygen weakly such that catalyst reoxidation becomes rate determining, activity will begin to decrease as the reduction potential increases. Then, as for other single reaction processes, catalyst *activity* will exhibit volcano behavior.

However, we can rarely treat oxidations as single reactions. Chemical catalysis is most often interested in *partial*

(or *selective*) oxidations, in which it is desirable to oxidize an organic feedstock to a partially oxidized product, rather than to combust it to carbon dioxide and water. At minimum, such processes must be described as sequential reactions A → B → C, in which the desired product is B. The optimum catalyst will no longer necessarily be the one that exhibits the highest rate for conversion of A to B, but rather one that favors A → B while disfavoring B → C, thus maximizing the *selectivity* (moles B produces per mole A reacted) or *yield* (moles B produced per mole A fed), depending on one's optimization criterion. In practice, selective oxidations are often characterized by triangular or series-parallel reaction networks. These add a parallel nonselective step, A → C, to the sequential reaction network above. The target is a catalyst that minimizes the impact of these nonselective steps while promoting the desired partial oxidation reaction.

It is worth recalling that selectivity will not usually be constant. For parallel reactions, selectivity will be independent of conversion only if the reaction orders with respect to reactant concentrations of the two parallel reactions are the same. For series reactions, selectivity will fall monotonically with increasing conversion, and yield will pass through a maximum at intermediate conversion, if both reactions in the sequence exhibit positive reaction orders. Thus when results are evaluated from different catalysts, it is often preferable to compare product yields rather than selectivities if the data have not been obtained at comparable reactant conversions.

How then should we expect the performance of oxidation catalysts to vary as we vary their reduction potentials? If catalyst reoxidation is not rate limiting, the activity of a family of catalysts for a single reaction would be expected to exhibit increasing activity with increasing reduction potential. Since there are no competing reactions in this simplest reaction scheme, selectivity would be constant (at 100%), and product yield would increase with increasing reduction potential, provided that the catalysts exhibited similar surface areas (site densities) and experiments were conducted at similar contact times. For a purely parallel reaction network, activity and yield would still increase monotonically with catalyst reduction potential (subject to the same assumptions above), provided that the reaction orders were the same for both reactions. In that case selectivity would again be constant, but it would not equal 100%, owing to the influence of the undesired, parallel side reaction. For a purely sequential reaction network, activity for oxidation of A will increase with increasing catalyst reduction potential, selectivity to B may be expected to decrease, and *yield* of B will pass through a maximum (i.e., exhibit volcano behavior) provided one samples a range of catalysts that range from the inactive but selective, to the active but nonselective.

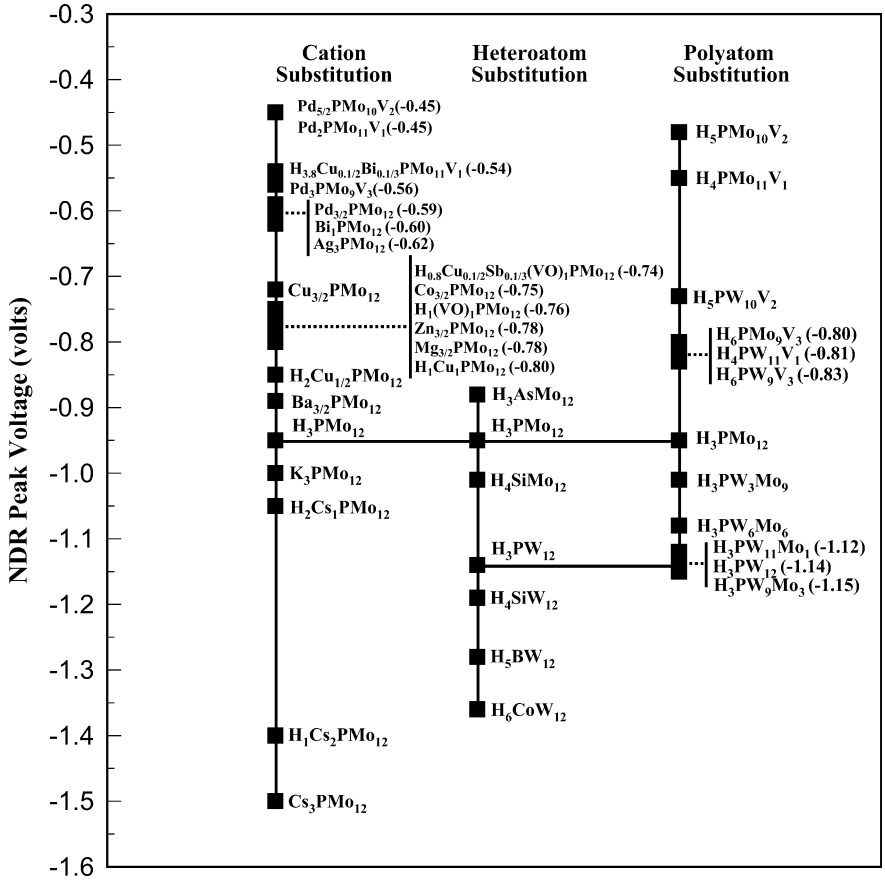

Fig. 4. Map of NDR peak voltages established for Keggin-type HPAs, along with classification according to the exchanged/substituted position.

The situation for series-parallel networks is a bit more complicated. If the reaction orders of the selective and nonselective reactions of A are the same, then the pattern of selectivity and yield vs reduction potential will be qualitatively similar to that outlined for purely series processes, but with the maximum selectivity achievable less than 100%. This assumes that relatively inactive catalysts (nonreducible materials in the case of oxidation catalysts) will still be selective. What is more likely is that they will open up completely different (nonselective from the point of view of oxidation catalysis) reaction paths. For example, nonreducible metal oxides often catalyze acid or base reactions. Thus if the span of catalysts considered includes materials that are not active for oxidation, one may observe increasing selectivity with increasing reduction potential, as oxidation becomes more competitive with other, undesired reactions. At some point within a family of increasingly potent oxidation catalysts the deleterious effect of sequential over-oxidation (B → C in the simple scheme above) may become significant, and selectivity will begin to decrease as reduction potential increases. In such a case reaction *selectivity* will exhibit volcano behavior as a function of catalyst reduction potential.

The scale of NDR peak potentials obtained from tunneling spectra of more than 40 HPAs [34], illustrated in Fig. 4, provides an unprecedented opportunity to evaluate this family of oxidation catalysts. As one examines oxidation processes that demand stronger or weaker oxidation catalysts, one might expect to see emerging the various patterns discussed above for the dependence of activity, selectivity, and yield on reduction potential (or NDR peak voltage). One can then hope to identify the reduction potential or NDR peak voltage associated with the "best" catalyst for the oxidation process of interest, and to search for related materials that exhibit similar NDR peaks. While experiments are needed that specifically target construction of volcano plots such as that illustrated in Fig. 3 (or other appropriate correlations of the types discussed earlier), the literature provides a sufficient base of reactivity data to begin to explore the strategies articulated here.

2. Single molecule spectra as correlating and predictive tools in selective oxidation by HPAs: case studies

One of the key issues in attempting to correlate catalytic performance with spectroscopy of model systems obtained ex situ is the stability of HPAs under catalytic reaction conditions. Even if one observes intact Keggin ions before and after reaction (as is often the case [50,51]), there is no guarantee that they operate in an intact state. However, their retention or recovery of a Keggin structure suggests that a close connection exists between their working and initial states, and that the characteristics of the latter may therefore provide useful correlating or predictive tools.

Thermal decomposition temperatures of potassium salts of simple phosphotungstate and phosphomolybdate Keggin ions are reported to exceed 350 °C [50,51]. When supported, these HPAs are often stable enough to survive the rigors of oxidations up to 380 °C or more [51]. Indeed it has been claimed that supporting heteropolyacids on their alkali salts increases their stability at elevated temperatures [51]. Unsupported HPAs are not as robust. Although phosphotungstates are more stable than phosphomolybdate Keggin ions, heating in the neighborhood of 400 °C often causes molecular rearrangements to occur [52–54]. This is particularly evident when vanadium is incorporated into the framework of a phosphomolybdate Keggin ion [54]. A recent study [55] investigating transient responses of the local electronic and geometric structures of $H_{3+x}PMo_{12-x}V_xO_{40}$ catalysts in selective oxidations showed that the vanadium migrated out of the Keggin anion into the cation-exchange position upon thermal treatment and/or chemical reduction during vapor phase oxidation reactions, producing a lacunary species characterized by defects in a number of metal-oxygen octahedra. This work concluded that the active state of the HPA was a partially reduced oligomer of polyanions bridged by vanadyl groups [55].

We consider below five case studies involving the use of supported HPAs to oxidize propane, butane, and isobutyric acid, and bulk HPAs to oxidize isobutane and acetaldehyde in the vapor phase. Relationships between catalyst performance and single molecule spectra obtained with the STM are explored for these five cases. Additional examples for which such relationships may be developed, including the oxidations of acrolein and ethylene with supported HPAs, and the oxidation of methane in the liquid phase by dissolved HPAs, will be the subject of future communications. While one might expect that the closest connections could be developed between the performance of supported HPA catalysts and spectroscopic measurements on supported HPA monolayers, to the extent that the latter reflect molecular properties, one may find utility for a broad range of conditions under which catalysis is carried out by discrete HPA molecules or assemblies or derivatives of them.

2.1. Oxidation of propane to acrylic acid

The oxidation of propane was carried out over a series of HPAs supported on a wide pore polyoxometalate [56] at 380 °C. Details of the oxidation procedure are given in US Patent 6,169,202. Results of these runs are given in Table 1 and form the basis of the volcano plot shown in Fig. 3. Fig. 5 adds the trends for conversion and selectivity vs NDR peak potential to this correlation. It is apparent from these additional data that the catalyst activity increases as the reduction potential increases (NDR peak potential becomes less negative), as expected. The selectivity is quite low for the least active catalyst, suggesting that parallel reactions control the selectivity for catalysts with insufficient oxidation activity. Selectivity increases rapidly for HPA catalysts with less negative NDR peak potentials reaching a maximum value near 30% for NDR values around −0.75

Table 1
The oxidation of propane to acrylic acid over heteropoly acids supported on a wide pore polyoxometalate [56]

HPA/$Cs_3PMo_{12}O_{40}$	Conversion (%)	AA Sel. (%)	AA yield (%)	NDR Peak Potential (V)
$H_3PMo_{12}O_{40}$	6.0	4.5	0.3	−0.95
$H_1(VO)PMo_{12}O_{40}$	27.0	28.4	7.8	−0.76
$H_{0.8}Cu_{0.1/2}Sb_{0.1/3}(VO)PMo_{12}O_{40}$	31.9	26.9	8.6	−0.74
$H_4PMo_{11}VO_{40}$	30.7	20.1	6.4	−0.55
$H_{3.8}Cu_{0.1/2}Bi_{0.1/3}PMo_{11}VO_{40}$	33.0	22.9	7.6	−0.54
$H_5PMo_{10}V_2O_{40}$	23.9	15.6	3.7	−0.48

to −0.5 V. Fig. 5 suggests a slight decline in selectivity for more active oxidation catalysts, generating the right-hand slope of the yield volcano in Fig. 3. The number of samples examined to date is probably not sufficient to conclude definitively whether selectivity passes through a maximum within the range of NDR peak potentials examined (the decrease in activity for $H_5PMoV_2O_{40}$ may reflect a support porosity problem, for example), but at the very least one can conclude that selective oxidation of propane to acrylic acid with HPA catalysts requires HPAs with characteristic NDR peaks above ca. −0.8 V.

2.2. Oxidation of isobutane to methacrylic acid, MAA, and methacrolein, MAL

Mizuno and coworkers [57] studied the oxidation of isobutane over a series of heteropolyacid catalysts at 340 °C. Table 2 and Fig. 6 summarize the results of this study, combined with our measurements of NDR peak potentials for the relevant HPAs. Although activity trends are unclear from this limited data set, both yield and selectivity increase as the reduction potential increases. Again this suggests that the poor selectivity of "weak" oxidation catalysts arises from parallel, nonselective reaction channels. Fig. 6 indicates that at an NDR peak potential of −0.5 V the maximum yield has not yet been reached, suggesting that even more active HPA catalysts (with less negative NDR peaks) might give superior performance. As shown in Fig. 4, incorporation of vanadium into the HPA framework, and exchange for the counterions with redox active metal cations such as Ag(I), Cu(II), and Pd(II) tend to shift the NDR peak potentials of phosphomolybdate heteropolyacids to less negative values.

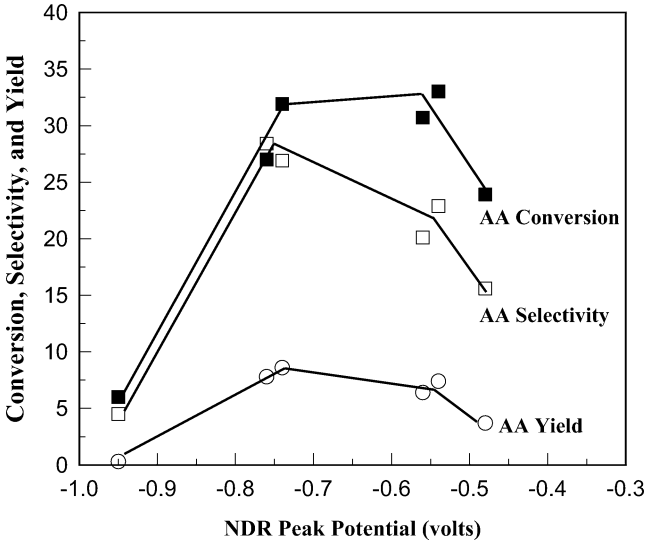

Fig. 5. Propane conversion, acrylic acid selectivity, and yield from [56] vs HPA NDR peak potentials for the experiments described in Fig. 3.

2.3. Oxidation of n-butane to maleic and acetic acids

Ai [58] studied the oxidation of *n*-butane at 360 °C to a mixture of maleic anhydride and acetic acid over Keggin ions supported on pumice. He reported product results as "acid" based on the mixture of maleic and acetic acids obtained by titration with NaOH. He noted that the ratio of maleic anhydride to acetic acid formed during oxidation holds steady at 0.6 ± 0.1. Table 3 and Fig. 7 compare the yields of these *n*-butane oxidation products as a function of the NDR peak potential of the HPA that was supported. These results suggest that while activity increases monotonically (even linearly) with NDR peak potential, the total acid selectivity remains nearly constant. If one considers the stability of the product acids, this result is perhaps not surprising. Oxidation activities beyond those of the HPAs represented in Table 3 would be required to produce significant overoxidation of the acid products of butane oxidation. Figs. 6 and 7 clearly show that for these two examples (oxidations of isobutane and butane), the available data are on the left leg of the "volcano," and that selectivity is limited primarily by parallel, nonselective reactions over the range of catalysts examined.

Table 2
Oxidation of isobutane to methacrylic acid and methacrolein over a series of heteropoly acid catalysts [57]

Catalyst	NDR (V)	S MAA (%)	S MAL (%)	Conv. (%)	Yld (%)[a]
$H_3PMo_{12}O_{40}$	−0.95	4	18	7	1.5
$H_6PMo_9V_3O_{40}$	−0.80	14	14	5	1.4
$H_4PMo_{11}VO_{40}$	−0.55	30	36	5	3.3
$H_5PMo_{10}V_2O_{40}$	−0.48	34	28	10	6.2

[a] Combined yields of MAA and MAL.

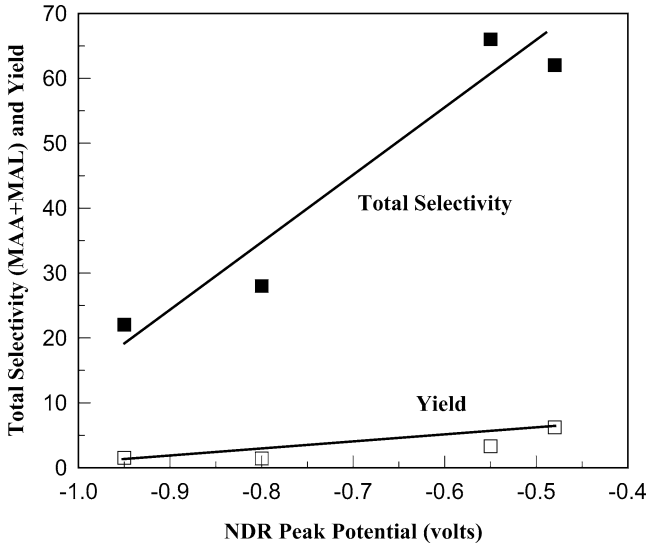

Fig. 6. Isobutane oxidation selectivity and yield to methacrylic acid (MAA) and methacrolein (MAL) from [57] vs HPA NDR peak potential.

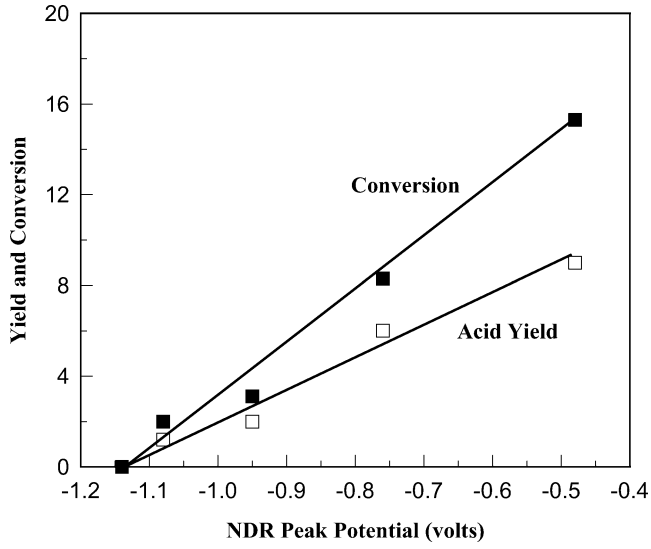

Fig. 7. Butane conversion and yield to acid products from [58] vs HPA NDR peak potential.

2.4. Oxidative dehydrogenation of isobutyric acid to methacrylic acid

A patent to ARCO [59] reported the oxidative dehydrogenation of isobutyric acid to methacrylic acid at 280 °C catalyzed by a series of Keggin ion HPAs supported on silica (Celite). Table 4 and Fig. 8 show the relationship between HPA NDR peak potentials on conversion, yield, and selectivity. There is a clear threshold value of the NDR peak potential in order for HPAs to carry out this oxidation. Conversion, selectivity, and yield all rise rapidly above this threshold, and for the limited data available, appear to plateau. It is important to note that the "plateau" conversion in Fig. 8 is >80% and varies little for HPAs with higher NDR peak potentials. Given the relatively high and invariant conversions reached with the phosphomolybdate HPAs in this study, it is not surprising that selectivity and yield do not vary significantly among this family of catalysts. More meaningful comparisons would require data to be obtained at lower conversions, where differences between active and selective catalysts might be better resolved.

Table 3
Comparison of conversion and yields of *n*-butane oxidation over a series of heteropolyacid catalysts [58] as a function of NDR peak potential

HPA/pumice	Acid yield (%)	Butane conv. (%)	NDR peak potential (V)
$H_3PW_{12}O_{40}$	0.0	0.0	−1.14
$H_3PW_6Mo_6O_{40}$	1.2	2.0	−1.08
$H_3PMo_{12}O_{40}$	2.0	3.1	−0.95
$H_1(VO)PMo_{12}O_{40}$	6.0	8.3	−0.76
$H_5PMo_{10}V_2O_{40}$	9.0	15.3	−0.48

2.5. Oxidation of acetaldehyde to acetic acid

The relatively easy oxidation of the weak C–H bond in aldehydes is catalyzed by most heteropolyacids [60] and is the reason the oxidation of methacrolein to methacrylic acid is performed industrially with such high yield and selectivity over HPA catalysts. The relative rates of the selective oxidation of acetaldehyde to acetic acid at 300 °C over a short series of HPAs as a function of their NDR peak potentials are given in Table 5 and Fig. 9. The trend in activity vs NDR peak potential is reminiscent of those in Figs. 5–8; there is a sharp rise in activity above a threshold NDR value, followed by a continuing monotonic increase that may or may not plateau.

2.6. Summary

Taken together, the results of these five case studies combining NDR peak potentials measured for HPA monolayers by STM, with literature data for catalyst performance, clearly show that less negative NDR peaks are associated with higher activity in oxidation catalysis. This is consistent with our previous demonstrations that NDR peak potentials for individual HPAs correlate with their reduction potentials

Table 4
Oxidative dehydrogenation of isobutyric acid to methacrylic acid over a series of heteropolyacid catalysts [59] as a function of their NDR peak potentials

HPA/SiO_2	NDR (V)	Conv. (%)	Sel. (%)	Yield (%)
$H_3PW_{12}O_{40}$	−1.14	0	0	0
$H_3PW_3Mo_9O_{40}$	−1.02	35	58	20
$H_3PMo_{12}O_{40}$	−0.95	82	44	36
$H_6PV_3Mo_9O_{40}$	−0.80	83	67	56
$H_4PVMo_{11}O_{40}$	−0.55	86	67	58
$H_5PV_2Mo_{10}O_{40}$	−0.48	85	70	60

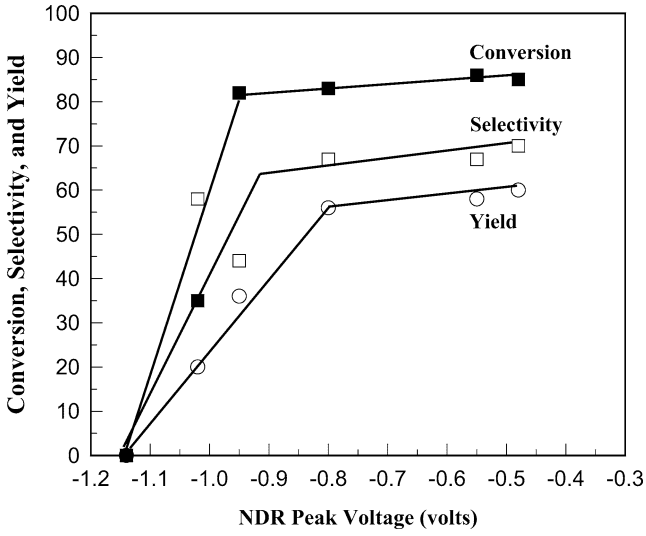

Fig. 8. Conversion, selectivity, and yield for oxidative dehydrogenation of isobutyric acid to methacrylic acid from [50] vs HPA NDR peak potential.

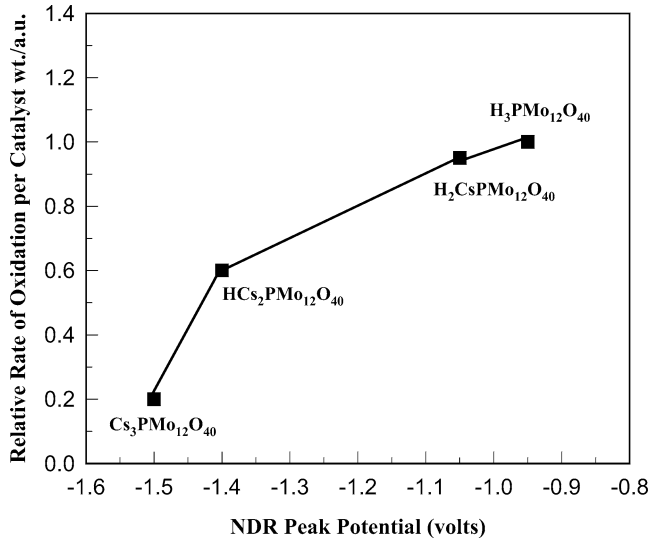

Fig. 9. Relative oxidation rates for conversion of acetaldehyde to acetic acid from [60] vs HPA NDR peak potential.

and illustrates the growing connection of results from single molecule spectroscopy to catalysis. The advantage of the comprehensive (and nearly continuous) scale of HPA NDR peak potentials is that it provides the tools to examine trends in catalyst activity, selectivity, and yield with a quantitative measure of the "oxidizing power" of these single site catalysts. Such trends may be used to interpret the structure of the reaction networks, as outlined earlier, to correlate catalyst performance with independently measured redox properties, *and to predict or select the optimum catalyst for the reaction of interest*. While the results to date are not sufficient to identify the optimum NDR values for HPA catalysts for different oxidation processes, they are consistent with the expectation that more difficult oxidations will require catalysts with higher reduction potentials/less negative NDR peak potentials. For example, extrapolation of the yield and selectivity curves in Figs. 5–9 to estimate the threshold value of the NDR peak potential required for each reaction produces the following order: propane (-0.95 V) > butane, isobutane, isobutyric acid (-1.1 to -1.2 V) > acetaldehyde (-1.55 V). This is in reasonable accord with the order of the strengths of the weakest C–H bonds in these molecules, which follow the order propane ∼ butane > isobutane > acetaldehyde. A similar picture is provided by comparing the conversion of different reactants with a single HPA. For example, the relative ease of the transformations: propane to propylene < propylene to acrolein < acrolein to acrylic acid, would indicate that the HPA-catalyzed oxidation of acrolein should be more efficient than propylene and the latter in turn would be more efficient than that of propane. Table 6 shows the yields of acrylic acid formed from each substrate when the oxidation is catalyzed by $H_4PMo_{11}VO_{40}$ supported on a polyoxometalate salt. In the sequence of oxidation steps taking propane to acrylic acid, conversion increases and the required operating temperature decreases when one starts with each successive oxidation product in the sequence, just as expected.

Table 5
Correlation between acetaldehyde oxidation rates [60] and NDR peak potentials

Catalyst	NDR peak potential (V)	Relative rate of oxidation
$H_3PMo_{12}O_{40}$	−0.95	1.00
$H_2CsPMo_{12}O_{40}$	−1.05	0.95
$HCs_2PMo_{12}O_{40}$	−1.40	0.60
$Cs_3PMo_{12}O_{40}$	−1.50	0.20

3. Conclusions

Metal oxides hold great promise for the molecular-level design of high selectivity catalysts for an enormous variety of processes. The key is to understand the reactivity of these materials at the molecular level, and to be able to fabricate surface features, both of model systems and of working catalysts, on the same scale. The formation of ordered monolayers of HPAs permits the characterization of these materials by tunneling spectroscopy. Negative differential resistance features in the tunneling spectra correlate well with the reduction potentials of these catalysts and serve as useful correlation and prediction tools for the performance of sup-

Table 6
Oxidation of substrates over a Keggin ion HPA supported on a POM salt[a]

Substrate oxidized	Run temperature (°C)	Acrylic acid yield (%)
Propane	380	6.4
Propylene	370	30.1
Acrolein	350	45.0

[a] Propane and propylene were oxidized under the same conditions [56] using $H_4PMo_{11}VO_{40}$ on $Cs_3PMo_{12}O_{40}$ while acrolein was oxidized [51] using this HPA on $K_3PMo_{12}O_{40}$.

ported HPA catalysts for selective oxidation processes. HPA monolayers thus present uniform catalytic sites whose redox properties can be defined by single molecule spectroscopy. They may serve as the prototype of single site heterogeneous catalysts designed and fabricated on the nanoscale.

References

[1] H. Cordatos, T. Bunleisen, J. Stubenrauch, J.M. Vohs, R.J. Gorte, J. Phys. Chem. 100 (1996) 785.
[2] S. Hilaire, X. Wang, T. Luo, R.J. Gorte, J. Wagner, Appl. Catal. A 215 (2001) 271.
[3] H. Hu, I.E. Wachs, S.R. Bare, J. Phys. Chem. 99 (1995) 10897.
[4] H. Hu, I.E. Wachs, J. Phys. Chem. 99 (1995) 10911.
[5] I.E. Wachs, B.M. Weckhuysen, Appl. Catal. A 157 (1997) 67.
[6] I.E. Wachs, Y. Cai, US Patent 6,350,918, Lehigh University, 2002.
[7] M.C. Libby, P.A. Watson, M.A. Barteau, Ind. Eng. Chem. Res. 33 (1994) 2904.
[8] P.C. Watson, M.C. Libby, M.A. Barteau, US Patent 5,475,144, University of Delaware, 1995;
M.A. Barteau, M.C. Huff, U. Pogodda, R. Martinez-Rey, US Patent 6,232,504, University of Delaware, 2001.
[9] R. Martinez, M.C. Huff, M.A. Barteau, Appl. Catal. A 200 (2000) 79.
[10] M.A. Barteau, Stud. Surf. Sci. Catal. 130 (2000) 105.
[11] M.A. Barteau, J. Vac. Sci. Technol. A 11 (1993) 2162.
[12] M.A. Barteau, Chem. Rev. 96 (1996) 1413.
[13] H. Idriss, M.A. Barteau, Adv. Catal. 45 (2000) 261.
[14] A.B. Sherrill, M.A. Barteau, in: D.P. Woodruff (Ed.), The Chemical Physics of Solid Surfaces, Vol. 4, Elsevier, Amsterdam, 2001, p. 409.
[15] K.I. Fukui, H. Onishi, Y. Iwasawa, Chem. Phys. Lett. 280 (1997) 296.
[16] A. Sasahara, H. Uetsuka, Onishi, Appl. Phys. A 72 (2001) S101.
[17] R.A. Bennett, P. Stone, R.D. Smith, M. Bowker, Surf. Sci. 454–456 (2000) 390.
[18] M. Li, W. Hebenstreit, U. Diebold, Phys. Rev. B 61 (2000) 4926.
[19] M. Li, W. Hebenstreit, U. Diebold, M.A. Henderson, D.R. Jennison, Faraday Discuss. 114 (1999) 245.
[20] R.E. Tanner, Y. Liang, E.I. Altman, Surf. Sci. 506 (2002) 251.
[21] M. Misono, Catal. Rev. Sci. Eng. 29 (1987) 269.
[22] C.L. Hill, C.M. Prosser-McCartha, Coord. Chem. Rev. 143 (1995) 407.
[23] B. Keita, L. Nadjo, J. Electroanal. Chem. 287 (1990) 149.
[24] J.T. Rhule, C.L. Hill, D.A. Judd, Chem. Rev. 98 (1998) 327.
[25] M. Misono, in: Y. Izumi, K. Urabe, M. Onaka (Eds.), Zeolite, Clay and Heteropolyacid in Organic Reactions, VCH, Weinheim, 1992, p. 99.
[26] N. Mizuno, M. Misono, Chem. Rev. 98 (1998) 199.
[27] M.S. Kaba, I.K. Song, D.C. Duncan, C.L. Hill, M.A. Barteau, Inorg. Chem. 37 (1998) 398.
[28] M. Ge, B. Zhong, W.G. Klemperer, A.A. Gewirth, J. Am. Chem. Soc. 118 (1996) 5812.
[29] B.A. Watson, M.A. Barteau, L. Haggerty, A.M. Lenhoff, R.S. Weber, Langmuir 8 (1992) 1145.
[30] B. Keita, L. Nadjo, Surf. Sci. 254 (1991) L443.
[31] I.K. Song, M.S. Kaba, G. Coulston, K. Kourtakis, M.A. Barteau, Chem. Mater. 8 (1996) 2352.
[32] M.S. Kaba, I.K. Song, M.A. Barteau, J. Phys. Chem. 100 (1996) 19577.
[33] I.K. Song, R.B. Shnitser, J.J. Cowan, C.L. Hill, M.A. Barteau, Inorg. Chem. 41 (2002) 2358.
[34] I.K. Song, J.E. Lyons, M.A. Barteau, Catal. Today, in press.
[35] M.S. Kaba, I.K. Song, M.A. Barteau, J. Phys. Chem. B 106 (2002) 2337.
[36] M. Kinne, M.A. Barteau, Surf. Sci. 447 (2000) 129.
[37] I.K. Song, M.S. Kaba, M.A. Barteau, J. Phys. Chem. 100 (1996) 17528.
[38] M.S. Kaba, I.K. Song, M.A. Barteau, J. Vac. Sci. Technol. A 15 (1997) 1299.
[39] M.S. Kaba, I.K. Song, D.C. Duncan, C.L. Hill, M.A. Barteau, Inorg. Chem. 37 (1998) 398.
[40] I.K. Song, M.S. Kaba, M.A. Barteau, W.Y. Lee, Catal. Today 44 (1998) 285.
[41] M.S. Kaba, M.A. Barteau, W.Y. Lee, I.K. Song, Appl. Catal. A 194 (2000) 129.
[42] I.K. Song, M.A. Barteau, Appl. Catal. A 182–183 (2002) 185.
[43] I.K. Song, M.S. Kaba, M.A. Barteau, Langmuir 18 (2002) 2358.
[44] I.K. Song, J. Kitchin, M.A. Barteau, Proc. Nat. Acad. Sci. 99 (2002) 6471.
[45] W. Stobbe-Kremers, M. van de Zon, J.J.F. Scholten, J. Catal. 154 (1995) 187.
[46] J.J. Altenau, M.T. Pope, R.A. Prados, H. So, Inorg. Chem. 14 (1975) 417.
[47] T. Okuhara, N. Mizuno, M. Misono, Adv. Catal. 41 (1996) 113.
[48] M. Sadakane, E. Steckhan, Chem. Rev. 98 (1998) 219.
[49] W.J.M. Rootsaert, W.M.H. Sachtler, Z. Phys. Chem. 26 (1960) 16.
[50] S. Damyanova, M. Cubeiro, J. Fierro, J. Mol. Catal. A 142 (1999) 85.
[51] K. Bruckman, J. Haber, E. Lalik, E. Serwicka, Catal. Lett. 1 (1988) 35.
[52] H.-S. Jiang, X. Mao, S.J. Xie, B.-K. Zhong, J. Mol. Catal. A 185 (2002) 143.
[53] G. Mestl, T. Ilkenhans, D. Spielbauer, M. Dieterle, O. Timpe, J. Krohnert, F. Jentoft, H. Knozinger, R. Schlogl, Appl. Catal. A 210 (2001) 12.
[54] C. Marchal-Roch, N. Laronze, N. Guillou, A. Teze, G. Herve, Appl. Catal. A 199 (2000) 33.
[55] G.K. Lee, S. Melsheimer, S. Berndt, G. Mestl, R. Schlogl, K. Kohler, Appl. Catal. A 214 (2001) 125.
[56] J.E. Lyons, A.F. Volpe, P.E. Ellis Jr., S. Karmakar, US Patent 5,990,348, 1999;
S. Karmakar, A.F. Volpe, P.E. Ellis Jr., J.E. Lyons, US Patent 6,043,184, 2000;
T.P. Wijesekera, J.E. Lyons, P.E. Ellis Jr., US Patents 6,060,419, 2000 and 6,169,202, 2001, assigned to Sunoco, Inc. and Rohm and Haas.
[57] N. Mizuno, Stud. Surf. Sci. Catal. 101 (1996) 1001. [And references therein.]
[58] M. Ai, in: Proc. 8th Intern. Congr. Catal., Berlin, Vol. 5, Chemie, Weinheim, 1985, p. 475.
[59] W.P. Shum, J.F. White, E.M. Beals, US Patent 4,522,934, Atlantic Richfield, 1985.
[60] N. Misono, N. Mizuno, H. Mori, K.Y. Lee, J. Jiao, T. Okuhara, Stud. Surf. Sci. Catal. 67 (1991) 87.